An Investigation of the Microstructure and Ductility of Annealed Cold-Rolled Tungsten

Chai Ren[1], Z. Zak Fang[1], Lei Xu[1], Jonathan P. Ligda[2], James D. Paramore[1,2], and Brady G. Butler[2]

Affiliations

[1]Department of Metallurgical Engineering, University of Utah, Salt Lake City, Utah, USA

[2]Lightweight and Specialty Metals Branch, U.S. Army Research Lab, Aberdeen Proving Ground, MD 21005, USA

Corresponding Author: zak.fang@utah.edu

Abstract

Tungsten is notoriously brittle metal at room temperature. Furthermore, contrary to most metals, plastic deformation increases ductility and recrystallization decreases ductility of tungsten. The fundamentals that govern this behavior have challenged academia and industry for decades. This paper focuses on understanding the controlling factors of ductility through a systematic investigation of the changes in microstructure and mechanical properties of cold-rolled tungsten that occur during annealing. Cold-rolled tungsten samples were annealed at temperatures up to 1400 °C, and mechanical testing and microstructural analysis was performed before and after annealing. Furthermore, a dislocation mobility model based on the Orowan equation was applied. The mechanisms of deformation are discussed within the context of deformed and annealed microstructures. The high fraction of low angle grain boundaries and high density of edge dislocations were found to be the most important factors for ductility. Although there were gradual changes in microstructure and mechanical properties, the ductility of cold-rolled tungsten was maintained up to 1300 °C. The material recrystallized when annealed above this temperature, had no ductility, and suffered brittle fracture. Microstructural

characterizations of the as-rolled material revealed a typical BCC texture, with grains elongated in rolling direction and a large amount of edge dislocations and low angle grain boundaries. The level of texturing and the fraction of low angle grain boundaries diminished after recrystallization. It was found that, compared to the recrystallized material, as-rolled tungsten can accommodate over 7 orders of magnitude higher deformation velocity due to the high density of edge dislocations.

Keywords: Tungsten, Ductility, Microstructure, Mechanical Properties, Annealing

1. Introduction

Body-centered cubic (BCC) metals are of great interest to both academic and industry researchers. The plasticity of BCC metals is fundamentally different from face-centered cubic (FCC) or hexagonal (HCP) metals [1]. Although plastic slip is expected in the close-packed <111> direction [2,3], specific slip planes in BCC metals are hard to define. The determination of specific slip planes varies based on applied stress and orientation [2], and slip may occur on planes that do not exhibit the maximum resolved shear stress [4]. This is a clear violation of Schmid's law, in which the primary slip system and critical resolved shear stress should be a constant for the same crystal system. Deformation studies on single crystals have shown several types of non-Schmid behaviors [4,5,6], and a number of slip planes have been reported for BCC metals, including {110}, {112} and {123} [7]. Among the BCC metals, tungsten is further unique. It not only exhibits a behavior that does not follow Schmid's law, but also defies several basic principles of materials processing and deformation mechanics. For example, contrary to classic work hardening theory, tungsten demonstrates improved ductility after cold working [8,9]. Tungsten is also known for having a solid solution softening effect when it is alloyed with Re. While this is a known phenomenon for some BCC metals [10,11], it is in contrast to solution

strengthening, which is more common for most metals. These characteristic behaviors make it both challenging and fundamentally important for understanding the mechanical properties of this highly refractory metal.

Tungsten is notoriously brittle at room temperature and has a high ductile-to-brittle transition temperature (DBTT). This causes serious difficulties in manufacturing and a number of end-use applications. Based on the fundamentals of dislocation theory, even restricting slip to only {110} type planes, there are 12 unique {110}<111> slip systems in tungsten. According to von Mises principle, a minimum of five independent slip systems is required to accommodate an arbitrary strain field during deformation of a polycrystalline material [12-15]. Taking this into consideration, the 12 unique {110}<111> slip systems will result in a total of 384 combinations of the required five independent slip systems [12,16]. From this aspect, tungsten is expected to be ductile, not brittle, as long as these slip systems are fully activated. Therefore, to explain the lack of ductility of tungsten, it is necessary to examine other microstructural features, such as grain boundaries, texture, dislocation character, and the availability of dislocation sources. In the past several decades, there has been a significant body of literature, mostly experimental studies, on improving the ductility of tungsten and decreasing its DBTT [17-23]. Among those works, thermomechanical processing is the most common and effective approach for improving the ductility of tungsten from none to substantial at a range of temperatures. One of the first reports of decreasing tungsten's DBTT by rolling was by G. Bodine and D. Maykuth in 1963 and 1964 [24,25]. After that, extensive research demonstrated that the ductility of rolled tungsten has a strong anisotropic behavior [26-28], and is very sensitive to the deformation ratio and rolling temperature [9, 29]. In today's industry, it is a standard practice to roll tungsten in multiple steps at a constant temperature or by gradually decreasing temperatures with each cycle. Using these

methodologies, the DBTT of tungsten can be reduced to less than 200 °C [27,30]. However, aside from the reports by J. Reiser et al. [28, 31] regarding the <110>||RD texture and large amount of low angle grain boundaries in cold-rolled tungsten, systematic studies on the correlation between microstructure and ductility of thermomechanically-processed tungsten are limited and sorely needed.

As discussed previously, the ductility of deformed tungsten can be completely lost by annealing at high temperatures, in contrast to the classical behavior of most metals. Both D. Terentyev et al. and J. Reiser et al. reported dramatic increases in DBTT and degradation of tensile strain after annealing cold-rolled tungsten at 1600 or 2000 °C [28,32]. This abnormal behavior of tungsten is important, because tungsten components are widely used in many high temperature applications, and thermal cycling is unavoidable during operation [33,34]. Therefore, understanding the effects of annealing on physical and mechanical properties of tungsten is essential to develop and design a new generation of tungsten-based components that are reliable in these particular applications.

In the present work, a detailed investigation was undertaken to study the evolution of the microstructure and ductility during annealing of rolled tungsten. The effects of annealing on microstructure, including grain boundaries, texture, dislocation density, ductility, and hardness, are presented herein. As such, the goal of this work is to understand the effects of microstructure on the ductility of tungsten. Furthermore, the mechanisms of deformation of tungsten are analyzed and discussed within the context of basic dislocation theory.

2. Experimental Procedure

2.1 Sample preparation

Commercially pure tungsten plate, manufactured by sintering tungsten powder and subsequent rolling, were purchased from Plansee. Samples had a reported purity of greater than 99.97%, with the content of each impurity element reported at less than 100 ppm. The purchased sheet had a microstructure that is characteristic of cold-rolling, thus it is referred to as cold-rolled tungsten in this work. Annealing of the cold-rolled tungsten was performed using an atmosphere-controlled tube furnace to study the effect of annealing temperature on the microstructure and mechanical behavior. All samples were heated at a rate of 5 °C/min and annealed at 300, 600, 800, 1000, 1200, 1300, 1350, and 1400 °C for 1 hour in argon (purity >99.995%).

2.2 Mechanical testing

Instrumented three-point bending tests were performed according to the ASTM C1211 Standard Test Method for Flexural Strength of Advanced Ceramics at Elevated Temperatures [35]. Small scale three-point bending unnotched specimens with dimensions of 46mm||RD, 4mm||ND, and 5mm||TD were electrical discharge machined (EDM) from the cold-rolled tungsten plate with loading direction parallel to the ND. Top and bottom sides of the sample retained the original rolled surface and the other two sides were tested with an EDM surface finish. The sample was positioned in such a way that the loading and supporting pins were in contact the rolled surfaces, which had a smoother surface finish. This was done because a smoother surface may improve the experimental accuracy and repeatability by minimizing the surface defects, which may function as crack initiation points. Further details about the effect of surface finish on mechanical behavior of cold-rolled tungsten can be found in a previous report [30] and the ASTM C1211 Standard [35].

During the test, the speed of the loading pin was 0.3 mm/min, which corresponded to a strain rate of 1.67×10^{-3} s^{-1} at the surface of the sample. The three-point bending fixture was placed

inside a furnace with a protective argon gas flow to minimize oxidation. To maintain a precise and stable test temperature, the specimens were heated together with the three-point-bending fixture inside furnace and kept at the desired temperature for at least 30 min before testing. Three thermocouples were placed next to the fixture to monitor the temperature gradient and ensure a stable and homogeneous testing temperature throughout the experiment. The three-point-bending tests were performed under displacement control mode. The test results, including displacement and load data, were recorded automatically by MTS Test Suite software and calculated based on the ASTM standard. Further details about this custom-designed, high-temperature, three-point-bending setup can be found in the literature [30].

Specimens for hardness analysis were polished using diamond suspensions down to 1 μm. Hardness of as-rolled and annealed tungsten was measured using a LECO LV700AT Vickers Hardness Tester with a load up to 30 kg on the polished surface of rolled sheet. At least 5 measurements were performed for each sample condition, and the average values are reported.

2.3 Microstructure analysis

The microstructures of as-rolled and annealed tungsten samples were characterized using a FEI Nova Nano scanning electron microscope (SEM). In order to measure grain size and shape, the tungsten samples were polished using diamond suspensions down to 0.25 μm. SEM images of the grain structure were taken on the polished surfaces, and grain sizes were determined using the linear intercept method. At least 300 intercepts of grains were measured parallel and perpendicular to the rolling direction, and at least 5 SEM micrographs from random and spread out locations were analyzed for each condition. The average grain size was calculated based on

the length of these intercepts. The grain shape aspect ratio was calculated by dividing the average width of grains by the average length of grains.

Electron backscatter diffraction (EBSD) measurements were performed using an FEI Nova NanoLab 600i SEM with an EDAX Hikari EBSD detector. The images were acquired using a 20 kV acceleration potential and 2.1 nA probe current. Areas of 45 x 60 μm were scanned with a step size of 100 nm for finer-grained samples. However, larger scan regions (170 x 225 μm) were required to obtain an adequate number of grains for texture and microstructural analysis of materials annealed at high temperatures. Grain boundaries with misorientation of <15° were considered low angle grain boundaries, while those with misorientation >15° were considered high angle grain boundaries.

The as-rolled and annealed tungsten foils for TEM analysis were extracted from the bulk samples using a focused ion beam (FIB) on a FEI Helios NanoLab 650 system. The foil specimens of about 200 nm in thickness were polished to electron transparency using a Fischione Model 1060 argon ion mill to remove potential surface damage during the FIB process. TEM analyses were performed using a JEOL JEM 2800 scanning transmission electron microscope (STEM) using bright field and dark field STEM at a 200 kV acceleration potential.

3. Results

3.1 Mechanical properties

3.1.1 Three-point bending results

Bending tests were conducted at 200 °C on the cold-rolled tungsten samples annealed at various temperatures. Figure 1 shows the three-point bending stress-strain curves of the various conditions. The DBTT of the as-received, cold-rolled, pure tungsten plate was observed in the

range of 150 to 200 °C, based on previous research [30]. Samples annealed at temperatures up 1300 °C showed ductile behavior with a maximum strain up to 0.18. The samples annealed at 1350 or 1400 °C had no ductility and failed at relatively low stress levels. The failure stress of these two samples are labeled as X-1350 and X-1400 in Figure 1. Additionally, the stress-strain curves are nearly flat beyond the elastic limit, which indicates that cold-rolled tungsten exhibits almost no strain hardening. Without the possibility of necking during a bending test, this is an interesting phenomenon exhibited by BCC metals during deformation and is consistent with previous reports [9, 36].

Figure 2 shows the effect of annealing temperature on the peak stress and maximum strain of the various conditions. Most of the peak stresses were taken at the yield point, while the samples annealed at 1350 and 1400 °C were taken at the point of failure. The maximum strains were taken as the flexural strain at failure. Based on the results, annealing temperatures up to 800 °C did not significantly affect the strength or the ductility of cold-rolled tungsten. As the annealing temperature increased above 800 °C, the peak stress gradually decreased and strain to failure increase up to 1300 °C. When the annealing temperature was above 1300 °C, rapid degradation of the maximum stress and strain was observed on the annealed samples. This abrupt change in ductility is attributed to recrystallization and grain growth. B. Allen et al. and K. Farrell et al. reported the recrystallization temperature of deformed tungsten at about 1250 °C [37,38], and S. Mathaudhu et al. reported a recrystallization temperature of about 1400 °C on their heavily deformed tungsten [39]. The results in the current work suggest the recrystallization temperature of this cold-rolled tungsten is between 1300 and 1350 °C. Figure 2 (b) also suggests that the ductility improved by annealing in the moderate temperature range of 800 to 1300 °C. To the authors' knowledge, this is the first time that this behavior has been reported in the literature.

3.1.2 Vickers hardness results

The Vickers hardness of cold-rolled tungsten after annealing at different temperatures is shown in Figure 3. The hardness decreased significantly from the as-rolled to the fully recrystallized condition. A closer inspection reveals that two different stages of softening can be seen, as indicated by the discontinuous trends. During the first stage, ranging from as-rolled to 1200 °C, the hardness decreased gradually with increasing annealing temperature. Above 1300 °C, a dramatic decrease in the hardness is observed. Based on SEM analysis, the second stage is attributed to recrystallization and grain growth, during which new grains nucleated and grew with drastically fewer dislocations. At temperatures below 1200 °C, the decrease in hardness during this stage is likely due to recovery of the highly deformed microstructure. The driving force for recovery and recrystallization is stored energy in the form of dislocations and low angle grain boundaries present in the deformed structure. The apparent difference between the recovery and recrystallization/grain growth stage is consistent with both our SEM characterization as well as work previously reported by A. Alfonso et al. [40,41].

3.2 Microstructural evolution

3.2.1 Grain size and morphology

The average grain sizes and grain aspect ratios as a function of annealing temperature are given in Figure 4 (a), (b) and (c). The average grain width showed no significant change as annealing temperature increased from as-rolled to 1200 °C. Further increasing the temperature led to recrystallization and growth and a rapid increase of the average grain width. Compared to width, average grain length remained almost constant at about 3350 nm, even after recrystallization and initial grain growth. Only a very slight change in the grain aspect ratio was

observed due to annealing at temperatures up to 1200 °C. However, at higher temperatures, grains grew through the thickness of the plate, resulting in a fully recrystallized and equiaxed morphology at 1400 °C.

3.2.2 Fracture surfaces

Figure 5 (a) shows the fracture surface of as-rolled tungsten, and Figure 5 (b) is the side surface of the as-rolled sample after the three-point bending test. Cracks developed during the bending test as the applied load increased. It appears that the cracks propagated perpendicular to the loading direction and along the elongated grains by intergranular fracture (as marked by white dotted rectangles). Some transgranular fracture was also observed through the layers of elongated tungsten grains (as marked by black dotted rectangles). This is consistent with previous studies performed by D. Rupp et al., which showed that the high angle grain boundaries in the rolling direction are the preferred crack paths [26].

Figure 6 compares fractographs of samples annealed at 800, 1200, and 1350 °C. The samples annealed at 800 and 1200 °C showed similar fracture behavior as the as-rolled sample, which includes elongated grains with laminate microstructure. The fracture surfaces contain mainly intergranular fracture along the rolling direction (as marked by white dotted rectangles) and some transgranular fracture through the deformed grains (as marked by black dotted rectangles). However, the sample annealed at 1350 °C fractured primarily in an intergranular fashion with coarse recrystallized grains showing near equiaxed polyhedral morphology. Additionally, the recrystallized sample had a straight crack path, which is a reflection of the stress distribution during three-point bending test. For samples annealed at lower temperatures, the fracture pathway was relatively straight near the surface with orientation parallel to loading direction. As the crack propagated away from the surface, its path deflected along the rolling direction. As

discussed in the last section, this deflection of the crack is not consistent with macroscopic loading stress, and this microscopic stress distribution can only be attributed to the laminate microstructure. Based on the analysis of the results shown in Figure 4 and Figure 6, annealing cold-rolled tungsten at temperatures above 1350 °C resulted in a more equiaxed microstructure, which is not effective for crack deflection during fracture.

3.2.3 EBSD analysis of texture and grain misorientation

Figure 7 (a) to (c) shows EBSD orientation maps of the as-rolled, 1200 °C annealed, and 1400 °C annealed conditions. Elongated grains can be observed in both the as-rolled and 1200 °C annealed samples. However, as the annealing temperature increased from 1200 to 1400 °C, the deformed grains recrystallized and grew, producing equiaxed grains with a larger average size. Areas of 45 x 60 μm were scanned with a step size of 100 nm for the as-rolled and 1200 °C annealed samples. However, larger scan regions (170 x 225 μm) were required to obtain an adequate number of grains for texture and microstructural analysis of samples annealed at 1400 °C. Compared to other factors, the effect of different scan areas on EBSD analysis is considered negligible.

The crystallographic textures of the as-rolled, 1200 °C annealed, and 1400 °C annealed materials are represented by pole figures shown in Figure 7 (d) to (f). The texture of cold-rolled tungsten has α (<110>||RD), γ (<111>||ND), and ε (<110>||TD) fiber components. The maps show that the strong {100} orientation preference on the pole figures is consistent through annealing up to 1400 °C. Furthermore, the other preferred orientation changed gradually after annealing, especially after the recrystallization and grain growth process at 1400 °C. The effect

of these preferred orientations on the mechanical behavior of cold-rolled tungsten will be discussed in the following sections.

In order to obtain more detail about the type and distribution of grain boundaries, the angles of grain boundaries were calculated based on the grain misorientations in the EBSD maps. Figure 8 (a) to (c) shows the distribution of grain boundaries in the same areas of EBSD mapping in Figure 7 (a) to (c). The grain boundary angle is marked by a color change from blue to red, corresponding to 2 to 60 degrees. The distributions of misorientation angle for all three conditions are shown in Figure 8 (d), where the number fraction is plotted against the misorientation angle. The as-rolled sample had a high number of low angle grain boundaries, especially in between the severely elongated grains with orientations close to {001} or {111} in the traverse direction. Only a very limited amount of high angle grain boundaries were observed. Annealing at 1200 °C led to no obvious change in the grain boundary distribution, with only a slight increase on the very low and very high angle regions. After 1400 °C annealing, the fraction of low angle grain boundaries decreased significantly, while the fraction of high angle grain boundaries increased. It has been reported that the high angle grain boundaries in rolled tungsten are the preferred crack path under a bending load [26]. Thus, considering crack propagation without the effects of local plasticity, the relatively low fraction of high angle grain boundaries limited the easy pathways for crack growth and increased the required energy to fracture. After annealing at high temperatures, a large amount of high angle grain boundaries were produced between equiaxed recrystallized and grown grains. This change in the overall degree of grain boundary misorientation eliminated the benefits of texture and introduced many easy paths for crack propagation. This at least partially explains the degradation of the facture toughness of cold-rolled tungsten after recrystallization and grain growth.

3.2.4 TEM analysis of dislocations and grain boundaries

Figure 9 shows TEM bright and dark field images of samples in the as-rolled, 1200 °C annealed, and 1400 °C annealed conditions, with the rolling direction marked by red arrows. All of the samples are represented with three images showing an overview, the dislocations, and a high-resolution image of the grain boundaries. The types and densities of dislocations were determined from the collected TEM images.

The overview TEM images of the three conditions shows consistent results with the previous SEM and EBSD analyses. No significant grain size and shape changes were found after annealing cold-rolled tungsten at 1200 °C. However, the tungsten annealed at 1400 °C showed recrystallized and grown grains with an equiaxed polyhedral morphology and larger average grain size. A large amount of dislocations can be easily observed in both the as-rolled and 1200 °C annealed grains, while the 1400 °C annealed sample contains only a limited amount of dislocations inside the grains.

A closer analysis reveals the existence of high density dislocation tangles and free dislocations inside the severely deformed tungsten grains in as-rolled condition. After 1200 °C annealing, the free dislocations are still present and uniformly distributed inside the grains, but the dislocation tangles are largely eliminated. The density of free dislocations was determined using the intercept method, which was $\sim 7.2 \times 10^{14}$ m^{-2} in the as-rolled condition, decreased to $\sim 1.9 \times 10^{14}$ m^{-2} after the 1200 °C anneal, and further decreased to only $\sim 1.1 \times 10^{12}$ m^{-2} after annealing at 1400 °C. In the as-rolled condition, free dislocations are a mixture of both edge and screw-types, of which the majority is the highly mobile edge-type (up to ~83% of the total dislocation length). The fraction of edge dislocations decreased slightly to ~75% after annealing at 1200 °C. This fraction further decreased and screw dislocations became predominant after

annealing at 1400 °C. This is understood as the higher-mobility edge dislocations cannot survive the sweeping of grain boundaries during high temperature annealing [42]. In the figures, edge dislocations are marked with black dotted rectangles, and screw dislocations are marked with white dotted rectangles. The corresponding Burgers vectors for the dislocations are also shown in the figures.

The high-resolution images show selected grain boundaries for each of the three conditions. Figure 9 (g) shows a low angle grain boundary in the as-rolled tungsten with limited lattice distortion. Figure 9 (h) and (i) show images of high angle grain boundaries in the 1200 °C and 1400 °C annealed samples. The locations of grain boundaries were determined based on distortion of the lattice and marked with red dotted lines.

Table 1 summarizes the results from the mechanical and microstructural analyses of the as-rolled, 1200 °C annealed, and 1400 °C annealed samples.

Table 1. Summary of mechanical and microstructure analysis results.

	As-rolled	1200 °C Annealed	1400 °C Annealed
Peak Stress (MPa)	1567	1366	664
Failure Strain (mm/mm)	0.110	0.162	0.003
Hardness (HV30)	501	472	395
Mean Grain Size (μm)	2.25	2.31	3.25
Grain Shape Aspect Ratio	3.2	2.7	1.2
Grain Boundary Angle	Mostly Low Angle	Mostly Low Angle	Mostly High Angle
Dislocation Density (m^{-2})	$7.2x10^{14}$	$1.9x10^{14}$	$1.1x10^{12}$
Dislocation Type	Mostly Edge	Mostly Edge	Mostly Screw

4. Discussion

As mentioned above, contrary to the basic principles of work hardening in metals, tungsten demonstrates a clear improvement in ductility after cold working. To understand this peculiarity of tungsten, this section will compare the fracture toughness and ductility of deformed and recrystallized tungsten. Based on the experimental results, grain boundaries and dislocations are discussed in detail. The large amount of low angle grain boundaries along with the rolling texture are determined to have a strong effect on tungsten's mechanical behavior. Modeling work, using the Orowan equation, shows that the high density of mobile edge dislocations also played an important role in cold-rolled tungsten's ductility.

4.1 Effects of the Grain Boundary Texture and Misorientation

Compared to as-sintered or recrystallized tungsten, cold-worked tungsten has a much higher density of grain boundaries as well as an increase in the relative number of low angle grain boundaries. Segregation of impurities like oxygen or phosphorous have been reported to significantly weaken the cohesion of tungsten grain boundaries, which results in poor ductility [43,44]. X. Wei et al. reported that due to the large amount of grain boundaries introduced during cold working, impurities in tungsten are redistributed and spread over a larger area [45, 46]. However, recent work by B. Gludovatz et al. has shown that intergranular fracture may not be directly correlated to the presence of impurities [47]. Therefore, other factors like grain shape or strain compatibility may play a more important role in determining the ductility of cold-rolled tungsten.

Based on the EBSD results, a large amount of low angle grain boundaries were generated during cold working. These low angle grain boundaries were stable through the low temperature annealing, but were removed during recrystallization and grain growth. This is consistent with a study reported by J. Reiser et al. [28]. This high ratio of low angle grain boundaries could improve the strain compatibility between tungsten grains. At low temperatures, the limited mobility of screw dislocations means that each of the slip systems is only partially active. If the total number of active independent slip systems is less than five, tungsten cannot accommodate the arbitrary strain field, which leads to high incompatibility between grains. During straining, cracks may nucleate and grow based on the strain incompatibility between grains, which leads to intergranular fracture. This is the reason for the extensive ductility of a tungsten single crystal [4], as there is no requirement to maintain compatibility between grains. Based on simulation work, Y. Cheng et al. reported that low angle grain boundaries between tungsten grains are able to transfer strain better without fracture, as it can effectively reduce the requirement of independent slip systems [48]. Three point bending tests of tungsten bi-crystals also showed that low angle grain boundaries have a higher fracture resistance compared to high angle grain boundaries [49]. Therefore, these results suggest that the high ratio of low angle grain boundaries observed in cold-rolled tungsten can significantly enhance strain compatibility between grains, thus improving ductility. It has long been postulated that low angle grain boundaries are stronger than high angle grain boundaries; however, the resistance to fracture may simply be the result of improved strain compatibility between neighboring grains.

The poor lattice coherency of high angle grain boundaries significantly increases the difficulty for dislocation migration and results in dislocation pile-ups and tangles. Dislocation tangles introduce local strains into the lattice, which may further impede the migration of

dislocations. Since the availability of dislocation sources and dislocation mobility at the crack tip are the two main factors affecting the DBTT of tungsten [50-53], the formation of dislocation tangles with no mobility would result in an increase of tungsten's DBTT. When compared to high angle grain boundaries, low angle grain boundaries have much more coherent crystal lattices and are basically equivalent to an array of dislocations at the boundary. The large ratio of low angle grain boundaries in cold-worked tungsten with a misorientation of <5° only introduce minor distortions to local crystal lattices. Selection rules for dislocation transfer at grain boundaries of different geometries have been reported by Clark at al. and Birnbaum et al. [54, 55, 56]. Boundaries that are parallel to both slip planes and directions are the most favorable orientation relationship for dislocation transfer. For conditions that are not parallel, the angle (θ) between the incoming and outgoing slip planes should be minimized. Dislocation transfer is unfavorable when θ is larger than 15° [54]. Based on these selection rules, for as-rolled and low temperature annealed samples, the high fraction of low angle grain boundaries with misorientation of <5° provided a close to ideal condition for dislocation transfer across grain boundaries. This accommodation of dislocation transfer reduced dislocation pileup, which has been shown to nucleate grain boundary cracks [57]. Similar effects of slip transfer across boundaries has been reported by Misra et al. on their studies of interphase and inter-metal boundaries [58, 59, 60]. Efficient slip transfer has been proved to be the key factor for the ~10 %EL ductility of their Ni-Fe-Al alloys at room temperature [59, 60]. Therefore, when compared to high angle grain boundaries, low angle grain boundaries can decrease tungsten's DBTT significantly.

Besides the frequency of low angle grain boundaries, microstructural morphology also has a strong effect on the mechanical properties of tungsten. As shown in Figure 3 of the as-rolled

condition, the elongated grains delaminated at the grain boundaries (intergranular fracture) along the direction parallel to deformation axis, and exhibited transgranular fracture along planes parallel to the loading direction. This fracture deflection effect of deformed tungsten may lead to more controllable crack growth during strain loading and result in higher fracture toughness [26,31]. Based on the EBSD maps and pole figures shown in Figure 10, cold-rolled tungsten samples showed significant α, γ, and ε fibers, with <110>||RD, <111>||ND, and <110>||TD textures, respectively. Annealing resulted in slightly lower intensities for each of these fibers. However, there is no significant change in the preferred orientations after recovery and recrystallization. The single notable exception is the shift in the maximum peak intensity away from the α-fiber described in Figure 10 (g). Tungsten is known to have a strong anisotropic behavior for fracture toughness, which is partly due to the difference in the fracture toughness reported for specific cleavage planes [61, 62]. The fracture behavior of polycrystalline tungsten is predominantly intergranular in nature [47]. Therefore, since the changes in texture are fairly small, a more pronounced reduction in fracture toughness would be expected based on the grain morphology of samples annealed at 1400 °C. Fully recrystallized samples do not show a strong propensity for crack deflection, which eventually results in catastrophic failure under strain loading.

4.2 Dislocation Density and Mobility

Dislocations are the key factor in the work hardening of metals. A high density of dislocations generated during plastic deformation impedes the movement of further dislocations, which results in strengthening of the metal and degradation in ductility. However, the plastic behavior of tungsten is inconsistent with this basic principle of work hardening, as tungsten has repeatedly demonstrated a clear improvement in ductility after cold working [9,24,28,30]. A

thorough understanding of the dislocation behavior is critical to understanding the general mechanical behavior of tungsten and other BCC metals that behave similarly.

Based on the TEM results discussed in the previous section, cold working tungsten generates a significant amount of dislocations, similar to most metals. Compared to the recrystallized material with significant grain growth, as-rolled tungsten had a more than two orders of magnitude higher free dislocation density and a considerable amount of dislocation tangles. Talia et al. studied the effects of surface oxide films on the mechanical behavior of single crystalline and polycrystalline tungsten and molybdenum materials [63, 64]. The surface films were reported to act as an efficient source of mobile non-screw dislocations, which resulted in notable ductility enhancement [63, 64, 65]. The significantly higher density of edge dislocations generated by cold working may function as extra dislocation sources in a similar fashion as the surface films, giving rise to improved ductility. Dislocation tangles are formed by interaction of dislocations during deformation of grains with ultrahigh dislocation density and limited dislocation mobility [66]. At high dislocation densities, these tangles impede dislocation motion and degrade the metal's ductility. On the other hand, when dislocation density is relatively low and the dislocations are less tangled, dislocation pile-ups at grain boundaries can function as dislocation sources, which is beneficial for the ductility of tungsten [64, 28].

Dislocations generated during the rolling process may have edge, screw, or mixed character, based on their orientation in the crystal lattice. Large differences have been found in the activation energies for the motion of screw and edge dislocations. The screw dislocation in BCC metals has an inherently compact and three-dimensional nature, which contributes to a relatively high Peierls barrier [67,68]. Formation of kink pairs is essential to the mobility of dislocations with this character [67], which is a thermally activated process. Therefore, a comparatively high

temperature is required to achieve mobility of screw dislocations under a reasonable applied stress [69]. In comparison, the activation energy for mobility of an edge dislocation is considerably lower. Therefore, these dislocations becomes active well below room temperature [70]. As the mobility of dislocations along the crack front is the most important factor to describing tungsten's DBTT, it can be expected that determining the difference between the motion of screw and edge dislocations is critical to explaining improved ductility in cold-rolled tungsten. Although the velocity of dislocations is difficult to measure experimentally, theoretical modeling based on the Orowan equation can be used to investigate dislocation mobility with regards to deformation velocity [71]:

$$\dot{\varepsilon} = b\rho_{\mathrm{m}} v_{\mathrm{dis}}(\tau, T), \quad (1)$$

where $\dot{\varepsilon}$ is the deformation velocity, b is the Burgers vector, ρ_{m} is the density of mobile dislocations, and $v_{\mathrm{dis}}(\tau, T)$ is the average dislocation velocity as a function of resolved shear stress and temperature (τ and T, respectively). By manipulating this equation, the deformation velocity can be calculated as a function of dislocation type, dislocation density, and deformation temperature. Further details about this model can be found in Appendix A, and the modeling results are discussed in the following section.

As shown in Figure 11 (a), the deformation velocity for both screw and edge dislocations are calculated using the Orowan equation as a function of dislocation density. For this analysis, the flow stress was fixed at 500 MPa, as this is a value just below any sample's failure point. Additionally, temperature was fixed at 200 °C, which is the testing temperature used in the current study. The calculated deformation velocity in tungsten with purely edge dislocations is 7 orders of magnitude faster than a sample with the same density of purely screw dislocations. Therefore, under the same conditions, and without considering changes in the density and

character of dislocations that occur during deformation, tungsten with a larger fraction of edge dislocations tends to have better overall dislocation mobility and deformation velocity. This, in turn, results in a lower DBTT and better ductility at a given strain rate. For both screw and edge dislocations, decreasing dislocation density from 7.2×10^{14} m^{-2} to 1.1×10^{12} m^{-2} results in a decrease in deformation velocity by nearly 3 orders of magnitude, thus reducing the overall ductility. Figure 11 (b) and (c) show another deformation velocity calculation for tungsten as a function of temperature with an as-rolled dislocation density of 7.2×10^{14} m^{-2} and a 500 MPa flow stress. Based on these results, an edge dislocation is active for migration at 0 °C or lower. However, a minimum temperature of 700 °C is required for a screw dislocation to have a comparable level of mobility. This is consistent with the simulation work reported by Po et al. [69] and the Charpy impact testing results by Reiser et al. [28].

Based on a comparison of experimental data with modeling results, it can be seen that as-rolled tungsten should have a large dislocation density with a majority of edge-type character. These high mobility edge dislocations may blunt crack tips by accommodating plasticity. As-rolled tungsten also contains a major fraction of low angle grain boundaries. The large fraction of low angle grain boundaries provide a close to ideal condition for dislocation transfer across grain boundaries, which limits both the dislocation pinning effect and nucleation of cracks at these boundaries. After annealing at 1400 °C, most of the highly active edge dislocations disappeared during the processes of recrystallization and grain growth. The dislocation density decreased drastically and screw dislocations became dominant. Compared to edge dislocations, screw dislocations have much lower mobility. The drop in dislocation density also decreases the ductility of tungsten due to the lack of dislocation sources. Additionally, after high temperature annealing, the majority of grain boundaries became high angle boundaries, which is not

favorable for dislocation transfer. As such, it is reasonable to state that the experimental and modeling results are consistent in explaining the sharp decrease in ductility after annealing at 1400 °C.

To conclude, grain boundary character, dislocation source, and dislocation mobility are all important factors controlling the ductility of tungsten. Low angle grain boundaries with nearly parallel slip planes and directions reduce intergranular strain and prevent the nucleation of grain boundary cracks. A high density of dislocation sources is beneficial for blunting crack tips and accommodating strain. Dislocation density and character determine the local effective strain rates that can be accommodated during deformation. High dislocation mobility accommodates deformation processes and controls crack growth. Therefore, in order to obtain good ductility and low DBTT in polycrystalline tungsten, a microstructure with a large fraction of low angle grain boundaries and a high density of edge dislocations is desired, which can be observed in the microstructure of cold-worked tungsten. After high-temperature annealing, the fraction of high angle grain boundaries increases, the total dislocation density decreases, and screw dislocations becomes more prevalent. Therefore, the ductility degrades significantly.

5. Summary

The present work focused on understanding the changes in microstructure and mechanical properties of cold-rolled pure tungsten as a function of the annealing temperature. Additionally, the factors that contribute to the ductility in deformed tungsten and the lack of ductility in recrystallized tungsten were discussed. To achieve this objective, the mechanical properties of a set of cold-rolled tungsten samples annealed at different temperatures were tested using three-point bending. Furthermore, the annealed microstructures were studied using a variety of characterization techniques, including SEM, TEM, and EBSD. The role of grain boundaries and

dislocations in the ductility and DBTT of tungsten were discussed based on both experimental and modeling results. The following can be summarized:

1) Annealing of cold-rolled tungsten at intermediate temperatures from 500 to 1200 °C didn't cause drastic changes in mechanical behavior. Although there were minor changes, the ductility remained relatively consistent. Annealing above 1350 °C caused recrystallization and grain growth, which lead to a dramatic loss in ductility and toughness.
2) As-rolled tungsten and samples annealed at moderate temperatures had a clear texture with α (<110>||RD), γ (<111>||ND), and ε (<110>||TD) fiber components, and elongated grains along the rolling direction. After high temperature annealing, the material was fully recrystallized, but maintained a texture that is typical of rolled BCC metals, with α, γ, and ε fibers. However, the overall intensity of the texture decreased. Additionally, grains became near-equiaxed polyhedrons by predominantly growing perpendicular to the rolling direction.
3) In the as-rolled samples and those annealed at moderate temperatures, a majority of grain boundaries had small angles of misorientation, while the recrystallized samples had a majority of high angle grain boundaries. The degree of misorientation plays a key role in accommodating strain across boundaries. That is, low angle grain boundaries are less likely to show brittle intergranular fracture, as boundary angles less than 15° are favorable for dislocations transfer. This improved dislocation mobility limited the pinning effect of grain boundaries on dislocation mobility, decreased dislocation pileup, and reduced nucleation of grain boundary cracks.

4) Dislocation density decreased gradually during annealing at low to moderate temperatures. However, it decreased sharply after recrystallization and grain growth. Edge dislocations were more prevalent in as-rolled and moderately annealed conditions. Screw dislocations became dominant after recrystallization and grain growth. The significantly higher density of edge dislocations generated by cold working may function as extra dislocation sources based on dislocation-dislocation interactions, thus leading to improved ductility.

5) A combination of factors, including the large fraction of low angle grain boundaries and a high density of edge dislocations, were responsible for the significantly better ductility of the cold-worked tungsten. The dominance of high angle grain boundaries and the overall lack of dislocations were responsible for the lack of ductility in the fully-recrystallized tungsten.

Acknowledgements

The authors wish to thank the U.S. Department of Energy (DOE), Office of Science, Fusion Materials Program (DESC0008673), SBIR program (DESC0017772), and the U.S. Department of Defense (DOD) SBIR program (W15QKN-13-C-0068) and (W15QKN-15-C-0038) for financial support. This work made use of the University of Utah USTAR shared facilities supported, in part, by the MRSEC Program of NSF under Award No. DMR-1121252. Additionally, this research was supported in part (JDP) by an appointment to the Postgraduate Research Participation Program at the US Army Research Laboratory (USARL) administered by the Oak Ridge Institute for Science and Education programs through an interagency agreement

between the US DOE and USARL. Particular thanks go to Prof. Siva Guruswamy for his invaluable assistance and comments.

Reference

[1] G. Taylor, C. Elam, The Distortion of Iron Crystals, Proc. R. Soc. A, 112 (1926) 337-361.

[2] J. Christian, Some Surprising Features of the Plastic Deformation of Body-Centered Cubic Metals and Alloys, Met. Trans. A, 14A (1983) 1237–1256.

[3] N. Chen, R. Maddin, Plasticity of Molybdenum Single Crystals, Trans. AIME, 191 (1951) 937–944.

[4] A. Argon, S. Maloof, Plastic Deformation of Tungsten Single Crystals at Low Temperatures, Acta Metall., 14 (1966) 1449-1462.

[5] C. Bolton, G. Taylor, Anomalous Slip in High-Purity Niobium Single Crystals Deformed at 77◦K in Tension. Philos. Mag. 26 (1972) 1359–76.

[6] H. Matsui, H. Kimura, Anomalous {110} Slip in High-Purity Molybdenum Single Crystals and Its Comparison with that in V(a) Metals, Mater. Sci. Eng. 24 (1976) 247–256.

[7] C. Weinberger, B. Boyce, C. Battaile, Slip Planes in BCC Transition Metals, Int. Mater. Rev., 58 (2013) 296-314.

[8] W. Coolidge, Ductile Tungsten, 249th Meeting of the American Institute of Electrical Engineers. New York: A.I.E.E. (1910) 961--965.

[9] Q. Wei, L. Kecskes, Effect of Low-Temperature Rolling on the Tensile Behavior of Commercially Pure Tungsten, Mater. Sci. Eng., A, 491 (2008) 62-69.

[10] W. Klopp, Review of Ductilizing of Group VIA Elements by Rhenium and Other Solutes, DTIC Document (1968).

[11] A. Luo, D. Jacobson, K. Shin, Solution Softening Mechanism of Iridium and Rhenium in Tungsten at Room Temperature, Int. J. Refract. Met. Hard Mater., 10 (1991) 107-114.

[12] W. Soboyejo, Mechanical Properties of Engineered Materials, CRC press (2002).

[13] R. von Mises, Mechanik der Plastischen Formänderung von Kristallen, Z. Angew. Math. Mech., 8 (1928) 161-185.

[14] G. Taylor, The Mechanism of Plastic Deformation of Crystals. Part II. Comparison with Observations, Proceedings of the Royal Society of London Series A, Containing Papers of a Mathematical and Physical Character 145 (1934) 388-404.

[15] G. Taylor, The Mechanism of Plastic Deformation of Crystals. Part I. Theoretical, Proc. Royal Soc. Lond., 145 (1934) 362-387.

[16] G. Groves, A. Kelly, Independent Slip Systems in Crystals, Philos. Mag. 8 (1963) 877-887.

[17] W. Klopp, W. Witzke, P. Raffo, Mechanical Properties of Dilute Tungsten-Rhenium Alloys, NASA Technical Note NASA TN D-3483, Washington, DC (1966).

[18] S. Wurster, B. Gludovatz, R. Pippan, High Temperature Fracture Experiments on Tungsten-Rhenium Alloys, Int. J. Refract. Met. Hard Mater., 28 (2010) 692-697.

[19] Y. Kitsunai, H. Kurishita, H. Kayano, Y. Hiraoka, T. Igarashi, T. Takida, Microstructure and Impact Properties of Ultra-Fine Grained Tungsten Alloys Dispersed with TiC, J. Nucl. Mater., 271-272 (1999) 423-428.

[20] C. Ren, Z. Fang, H. Zhang, M. Koopman, The Study on Low Temperature Sintering of Nano-Tungsten Powders, Int. J. Refract. Met. Hard Mater., 61 (2016) 273-278.

[21] C. Ren, M. Koopman, Z. Fang, H. Zhang, B. van Devener, A Study on the Sintering of Ultrafine Grained Tungsten with Ti-Based Additives, Int. J. Refract. Met. Hard Mater., 65 (2017) 2-8.

[22] Q. Wei, H. T. Zhang, B. E. Schuster, et al., Microstructure and Mechanical Properties of Super-Strong Nanocrystalline Tungsten Processed by High-Pressure Torsion, Acta Mater., 54 (2006) 4079-4089.

[23] B. Gludovatz, S. Wurster, A. Hoffmann, R. Pippan, Fracture Toughness of Polycrystalline Tungsten Alloys, Int. J. Refract. Met. Hard Mater., 28 (2010) 674-678.

[24] G. Bodine, Tungsten Sheet Rolling Program, Final Report, Fansteel Metallurgical Corp., North Chicago, Illinois (1963).

[25] D. Maykuth, The Production of Powder-Metallurgy Tungsten Sheet and Plate, DMIC Memorandum, Battelle Memorial Institute (1964).

[26] D. Rupp, R. Monig, P. Gruber, S. Weygand, Fracture Toughness and Microstructural Characterization of Polycrystalline Rolled Tungsten, Int. J. Refract. Met. Hard Mater.,28 (2010) 669–673.

[27] T. Shen, Y. Dai, Y. Lee, Microstructure and Tensile Properties of Tungsten at Elevated Temperatures, J. Nucl. Mater., 468 (2016) 348-354.

[28] J. Reiser, J. Hoffmann, U. Jantsch, M. Klimenkov, S. Bonk, C. Bonnekoh, M. Rieth, A. Hoffmann, T. Mrotzek, Ductilisation of Tungsten (W): On the Shift of the Brittle-to-Ductile Transition (BDT) to Lower Temperatures Through Cold Rolling, Int. J. Refract. Met. Hard Mater., 54 (2016) 351–369.

[29] X. Zhang, Q. Yan, S. Lang, M. Xia, C. Ge, Texture Evolution and Basic Thermal-Mechanical Properties of Pure Tungsten Under Various Rolling Reductions, J. Nucl. Mater., 468 (2016) 339-347

[30] H. Zhang, The Effect of Ultrafine-grain Size and Titanium Hydride Addition on Mechanical Properties of Tungsten, Master Thesis, University of Utah 2017.

[31] J. Reiser, S. Wurster, J. Hoffmann, S. Bonk, C. Bonnekoh, D. Kiener, R. Pippam, A. Hoffmann, M. Rieth, Ductilisation of Tungsten (W) Through Cold-Rolling: R-Curve Behavior, Int. J. Refract. Met. Hard Mater., 58 (2016) 22–33.

[32] D. Terentyev, X. Xiao, A. Dubinko, A. Bakaeva, H. Duan, Dislocation-Mediated Strain Hardening in Tungsten: Thermo-Mechanical Plasticity Theory and Experimental Validation, J. Mech. Phys. Solids 85 (2015) 1–15.

[33] A. Suslova, O. El-Atwani, D. Sagapuram, S. Harilal, A. Hassanein, Recrystallization and Grain Growth Induced by ELMs-Like Transient Heat Loads in Deformed Tungsten Samples, Sci. Rep., 4 (2014) 6845.

[34] G. Pintsuk, Tungsten as Plasma Facing Material, Compr. Nucl. Mater., 4 (2012) 551-581.

[35] ASTM Standard C1211, Standard Test Method for Flexural Strength of Advanced Ceramics at Elevated Temperatures, ASTM International, West Conshohocken, PA (2018).

[36] M. Battabyal, R. Schaulin, P. Spatig, N. Baluc, W-2wt.%Y2O3 Composite: Microstructure and Mechanical Properties, Mater. Sci. Eng., A, 538 (2012) 53-57.

[37] B. Allen, D. Maykuth, R. Jaffee, The Recrystallization and Ductile-Brittle Transition Behavior of Tungsten. Effect of Impurities on Polycrystals Prepared from Single Crystals, J. Inst. Met. 90 (1961) 120–128.

[38] K. Farrell, A. Schaffhausen, J. Stiegler, Recrystllization, Grain Growth and the Ductile-Brittle Transition in Tungsten Sheet, J. Less-Common Met. 13 (1967) 141–155.

[39] S. Mathaudhu, A. de Rosset, K. Hartwig, L. Kecskes, Microstructures and Recrystallization Behavior of Severely Hot-Deformed Tungsten, Mater. Sci. Eng., A, 503 (2009) 28-31.

[40] A. Alfonso, D. Juul Jensen, G. Luo, W. Pantleon, Thermal Stability of a Highly-Deformed Warm-Rolled Tungsten Plate in the Temperature Range 1100-1250 C, Fusion Eng. Des., 98-99 (2015) 1924-1928.

[41] A. Alfonso, D. Jensen, G. Luo, W. Pantleon, Recrystallization Kinetics of Warm-Rolled Tungsten in the Temperature Range 1150-1350 C, J. Nucl. Mater., 455 (2014) 591-594.

[42] D. Hull, D. Bacon, Introduction to Dislocations, Butterworth-Heinemann, Woburn, 2001.

[43] E. Lassner, W. Schubert, Tungsten—Properties, Chemistry, Technology of the Element, Alloys, and Chemical Compounds, Springer, Berlin, 1999.

[44] Tran-Huu-Loi, J. Morniroli, M. Gantois, M. Lahaye, Brittle Fracture of Polycrystalline Tungsten, J. Mater. Sci. 20 (1985) 199.

[45] Q. Wei, K. Ramesh, E. Ma, L. Kesckes, R. Dowding, V. Kazykhanov, R. Valiev, Plastic Flow Localization in Bulk Tungsten with Ultrafine Microstructure, Appl. Phys. Lett. 86 (2005) 101907.

[46] Q. Wei, T. Jiao, K. Ramesh, E. Ma, L. Kecskes, L. Magness, R. Dowding, V. Kazykhanov, R. Valiev, Mechanical Behavior and Dynamic Failure of High-Strength Ultrafine Grained Tungsten Under Uniaxial Compression, Acta Mater. 54 (2006) 77-87.

[47] B. Gludovatz, S. Wurster, T. Weingärtner, A. Hoffmann, R. Pippan, Influence of Impurities on the Fracture Behaviour of Tungsten, Philos. Mag., 91 (2011) 3006-3020.

[48] Y. Cheng, M. Mrovec, P. Gumbsch, Atomistic Simulations of Interactions Between the 1 / 2<111> Edge Dislocation and Symmetric Tilt Grain Boundaries in Tungsten, Philos. Mag., 88 (2008) 547-560.

[49] E. Smiti, P. Jouffrey, A. Kobylanski, The Influence of Carbon and Oxygen in the Grain Boundary on the Brittle-Ductile Transition Temperature of Tungsten Bi-Crystals, Scr. Metall., 18 (1984) 673-676.

[50] A. Hartmaier, P. Gumbsch, Mesoscopic Simulation of Dislocation Activity at Crack Tips, MRS Proceedings 539 (1998) 233-44.

[51] P. Hirsch, S. Roberts, Modelling Plastic Zones and the Brittle-Ductile Transition, Phil. Trans. Roy. Soc. Lond. A355 (1997) 1991-2001.

[52] J. Rice, R. Thomson, Ductile Versus Brittle Behavior of Crystals, Phil. Mag. 29 (1973) 73-97.

[53] S. Roberts, Modelling Brittle-Ductile Transitions. In: Lépinoux J., Mazière D., Pontikis V., Saada G. (eds) Multiscale Phenomena in Plasticity: From Experiments to Phenomenology, Modelling and Materials Engineering. NATO Science Series (Series E: Applied Sciences), 367. Springer, Dordrecht (2000).

[54] Z. Shen, R. Wagoner, W. Clark, Dislocation and Grain Boundary Interactions in Metals, Acta Met. 36 (1988) 3231-3242.

[55] W. Clark, R. Wagoner, Z. Shen, T. Lee, I. Robertson, H. Birnbaum, On the Sriteria for Slip Transmission Across Interfaces in Polycrystals, Scr. Met. 26 (1992) 203-206.

[56] T. Lee, I. Robertson, H. Birnbaum, An In-Situ Transmission Electron Microscope Deformation Study of the Slip Transfer Mechanisms in Metals, Metall. Trans. 21A (1990) 2437-2447.

[57] I. Robertson, T. Lee, R. Subramanian, H. Birnbaum, Structure and Properties of Interfaces in Materials, MRS Symposia Proceedings, Materials Research Society, Pittsburgh, PA, 238 (1992) 357-367.

[58] A. Misra, R. Gibala, Slip Transfer and Dislocation Nucleation Processes in Multiphase Ordered Ni-Fe-Al Alloys, Metall. Mater. Trans. A 30A (1999) 991-1001.

[59] A. Misra, R. Gibala, Room-Temperature Deformation Behavior of Directionally, Solidified Multiphase Ni-Fe-Al Alloys, Metall. Mater. Trans. A 28 (1997) 795-807.

[60] R. Noebe, A. Misra, R. Gibala, Plastic Flow and Fracture of B2 NiAl-based Intermetallic Alloys Containing a Ductile Second Phase, ISIJ International 30 (1991) 1172-1185.

[61] D. Hull, P. Beardmore, A.P. Valentine, Crack Propagation in Single Crystals of Tungsten, Philos. Mag. 12 (1965) 1021.

[62] J. Riedle, P. Gumbsch, H.F. Fischmeister, Cleavage Anisotropy in Tungsten Single Crystals, Phys. Rev. Lett. 76 (1996) 3594.

[63] J. Talia, L. Fernandez, R. Gibala, Surface Oxide Softening in Tungsten and Molybdenum Single Crystals, Scr. Met. 12 (1978) 737-740.

[64] T. Tottori, J. Talia, R. Gibala, Surface Oxide Softening of Polycrystalline Molybdenum and Tungsten, Scr. Met. 14 (1980) 1153-1155.

[65] V. Sethi, R. Gibala, Surface Oxide Softening of Nb and Ta Single Crystals, Scr. Met. 9 (1975) 527-532.

[66] H. Wilsdorf, J. Schmitz, The Observation and Interpretation of Dislocation Tangles in the Easy Glide Range of Aluminum, J. Appl. Phys. 33 (1962) 1750.

[67] P. Hirsch, Comment, in Proc. 5th Int. Conf. Crystallography, Cambridge University (1960) 139.

[68] A. Groger, V. Vitek, Multiscale Modeling of Plastic Deformation of Molybdenum and Tungsten: I. Atomistic Studies of the Core Structure and Glide of ½<111> Screw Dislocations at 0 K, Acta Mater., 56 (2008) 5401-5411.

[69] G. Po, Y. Cui, D. Rivera, D. Cereceda, T. Swinburne, J. Marian, N. Ghoniem, A Phenomenological Dislocation Mobility Law for BCC Metals, Acta Mater., 19 (2016) 123-135.

[70] M. Duesbery, W. Xu, The Motion of Edge Dislocations in Body-Centered Cubic Metals, Scr. Mater., 39 (1998) 283-287.

[71] A. Hartmaier, Modeling of Crack-Tip Plasticity in Tungsten Single Crystals, Thesis, Max-Planck-Institute Fur Metallforschung, Stuttgart, 2000.

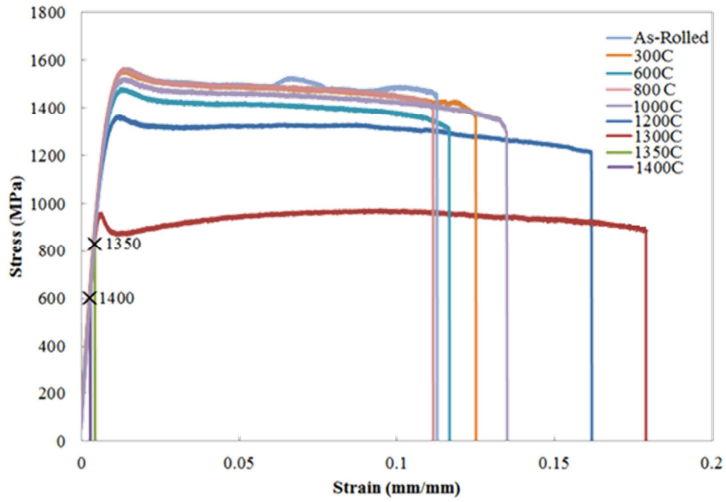

Figure 1. Engineering stress-strain curves of cold-rolled tungsten annealed at different temperatures and tested by three-point bending at 200 °C.

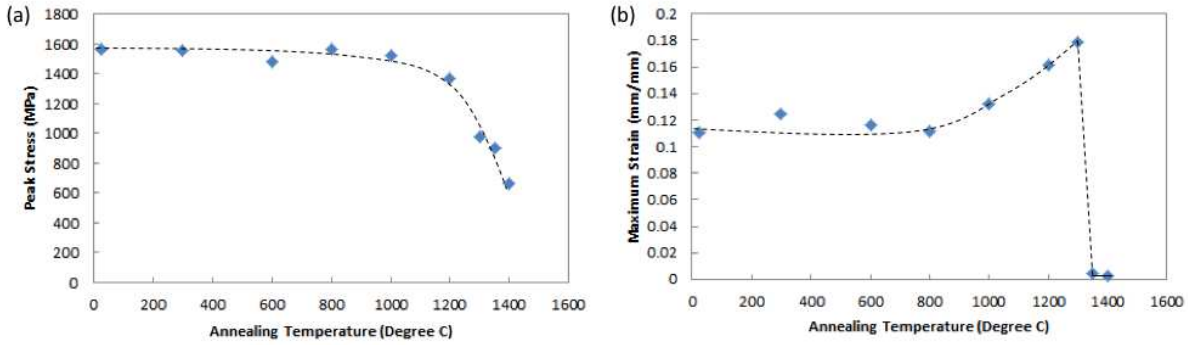

Figure 2. Effect of annealing temperature on the (a) peak stress and (b) maximum strain of cold-rolled tungsten during three-point bending tests at 200 °C.

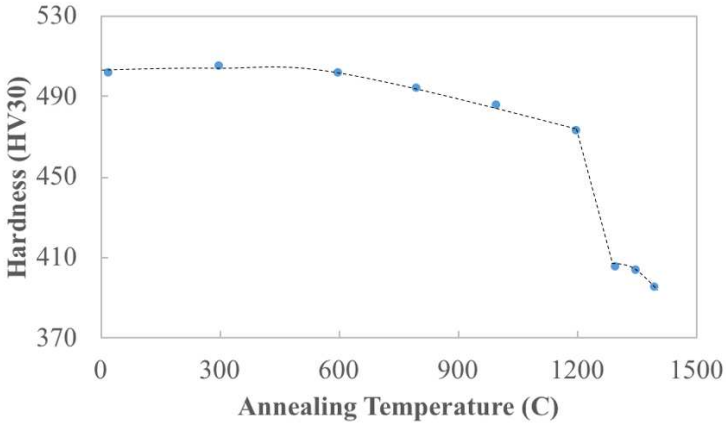

Figure 3. Evolution of Vickers hardness of cold-rolled tungsten with different annealing temperatures.

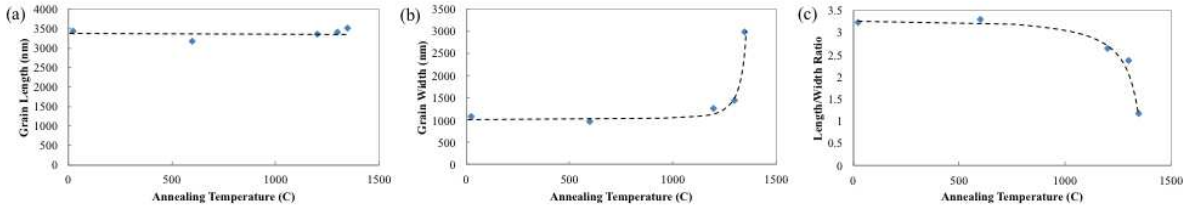

Figure 4. Effect of annealing temperature on the average (a) grain length, (b) grain width, and (c) length to width aspect ratio of cold-rolled tungsten.

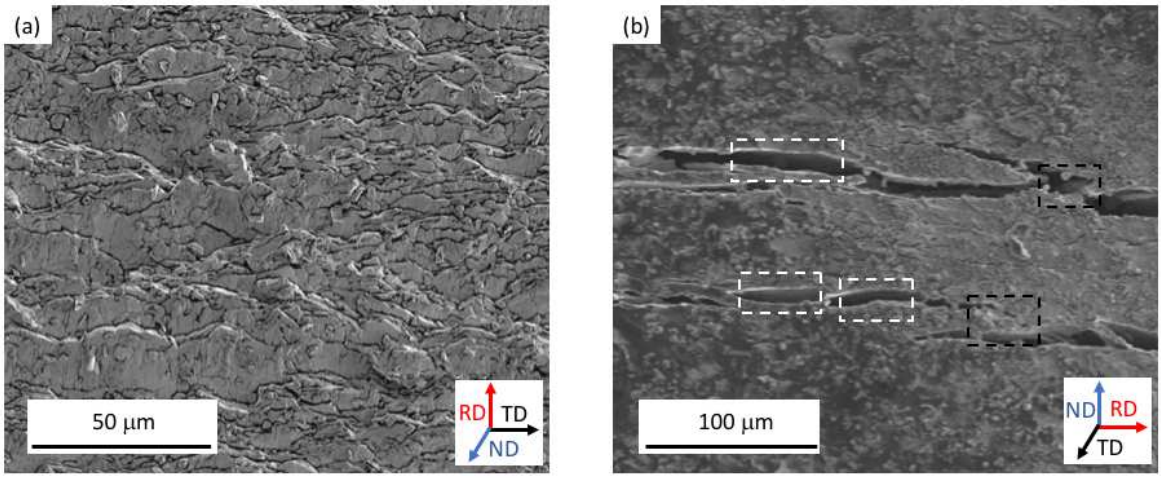

Figure 5 (a) Fracture surface of as-rolled tungsten after three-point bending test, (b) side surface showing crack propagation with increasing applied load during the 3-point bending test.

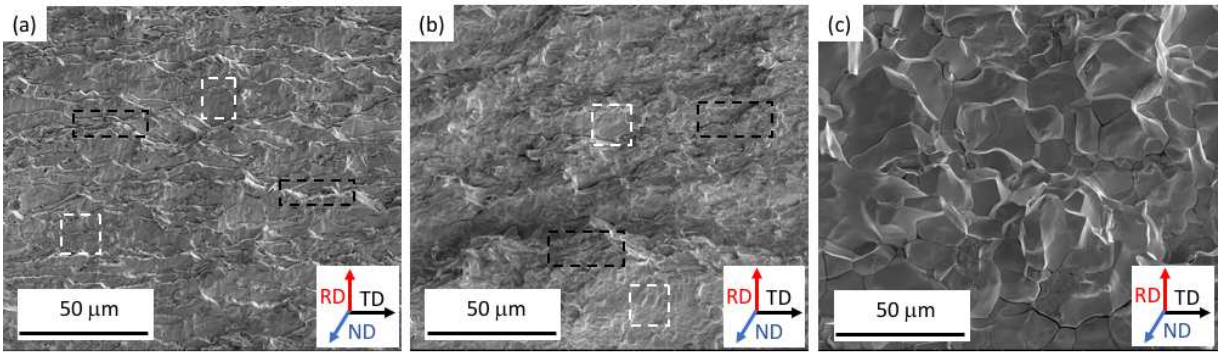

Figure 6 SEM fracture surfaces of cold-rolled tungsten after three-point bending tests with annealing temperatures of (a) 800 °C, (b) 1200 °C, (c) and 1350 °C.

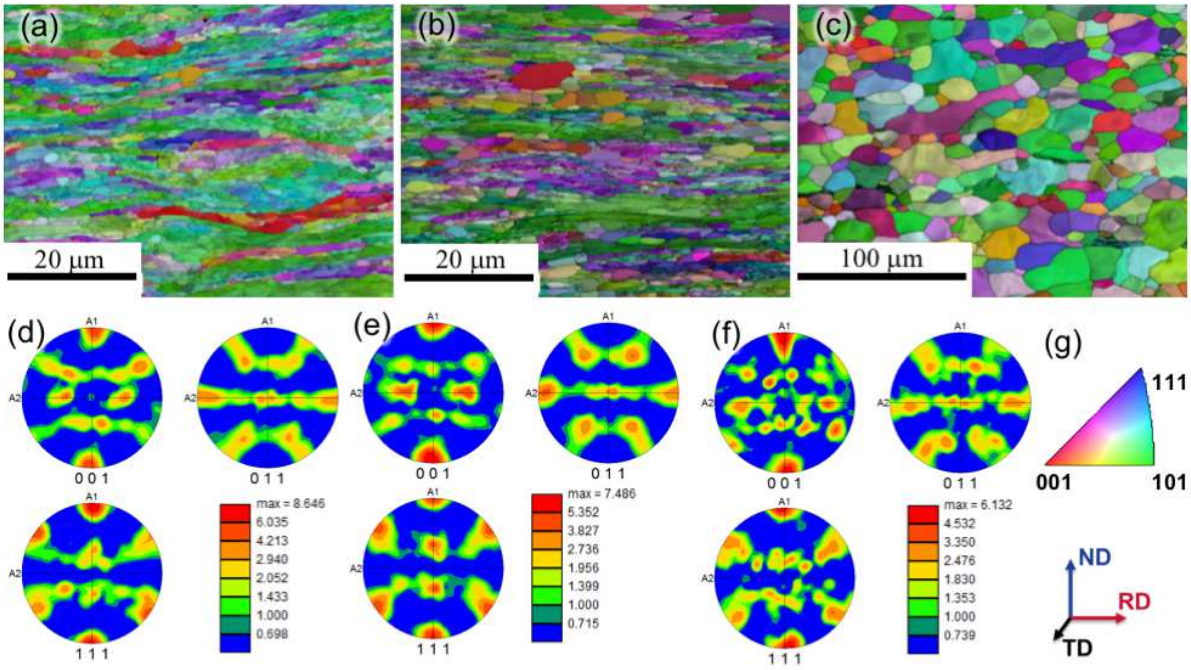

Figure 7 EBSD Mapping of the (a) as-rolled, (b) 1200 °C annealed, and (c) 1400 °C annealed cold-rolled tungsten, and selected pole figures of the (d) as-rolled, (e) 1200 °C annealed, and (f) 1400 °C annealed samples; (g) coloring and coordinate system for orientation maps shown in (a)-(c).

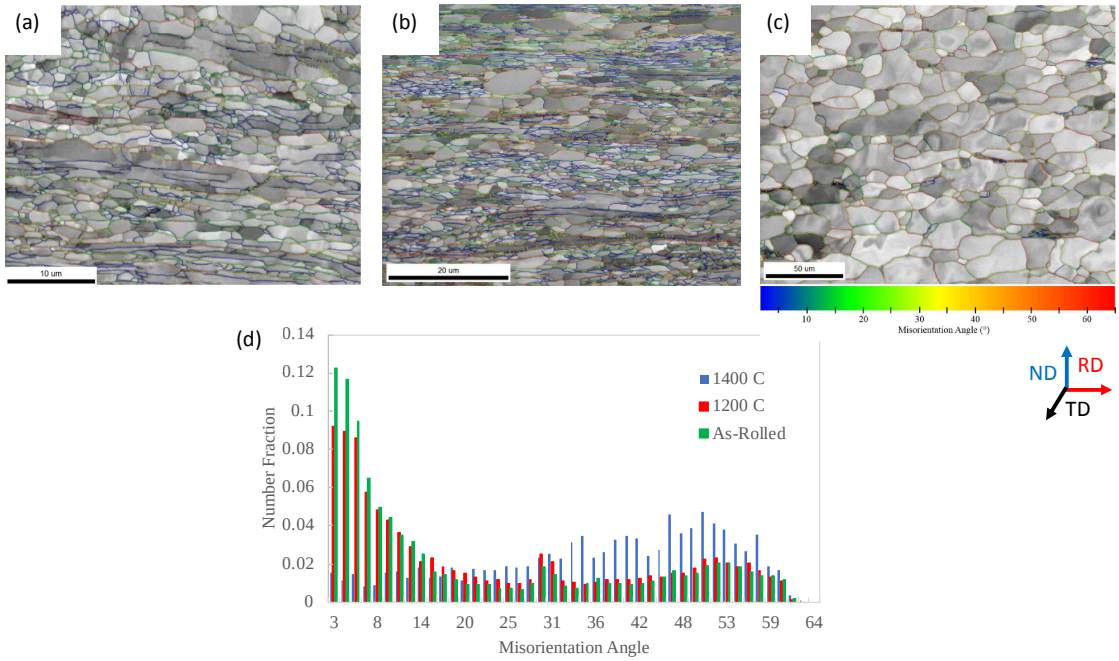

Figure 8. EBSD grain boundary maps of the (a) as-rolled, (b) 1200 °C annealed, and (c) 1400 °C annealed tungsten, (d) distribution of misorientation angle of the three annealed conditions.

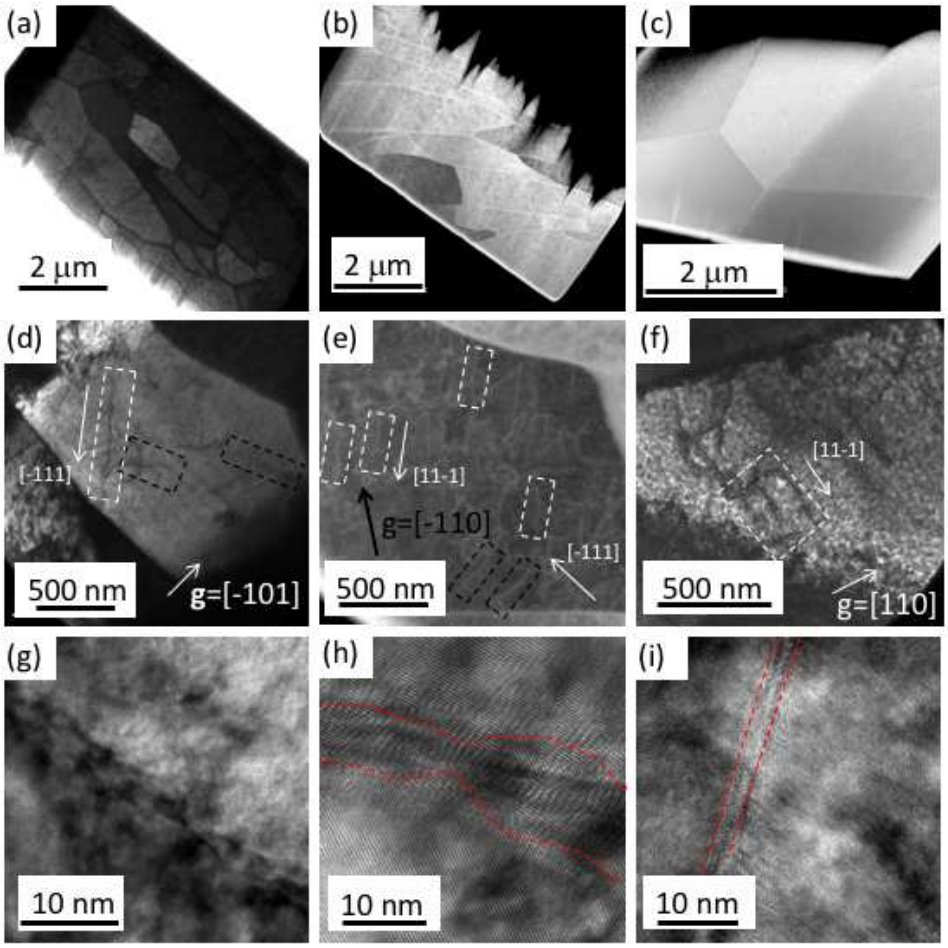

Figure 9. TEM images of cold-rolled tungsten in the as-rolled, 1200 °C annealed, and 1400 °C annealed conditions: (a to c) overview, (d to f) dislocation structure, (g to i) grain boundaries. (a), (g), (h), (i) bright field; (b), (c), (d), (e), (f) dark field; (c), (d), (e), (f) STEM mode; (a), (b), (g), (h), (i) TEM mode.

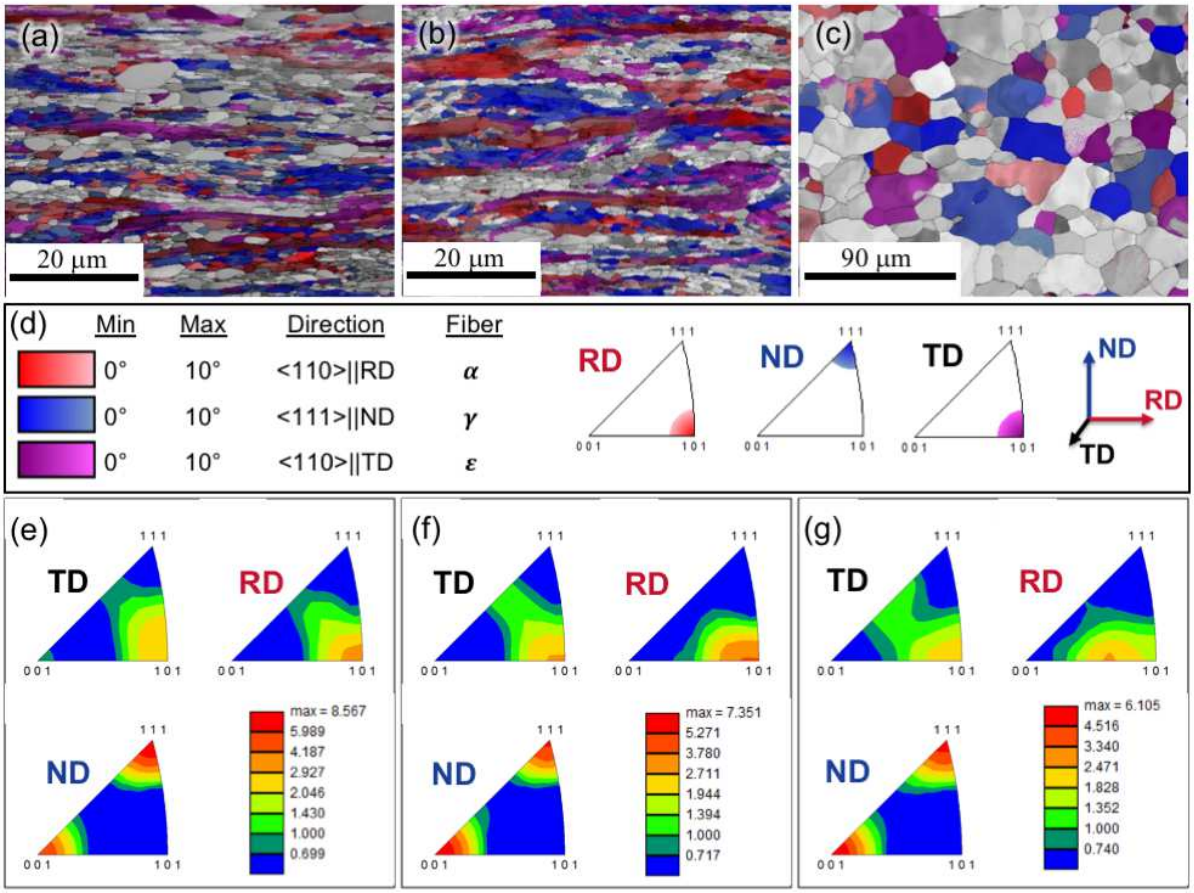

Figure 10. Texture and common BCC rolling fibers in (a) as-rolled, (b) 1200 °C annealed, and (c) 1400 °C annealed conditions; (d) legend for (a) to (c); (e) to (g) inverse pole figures corresponding to the maps in (a) to (c).

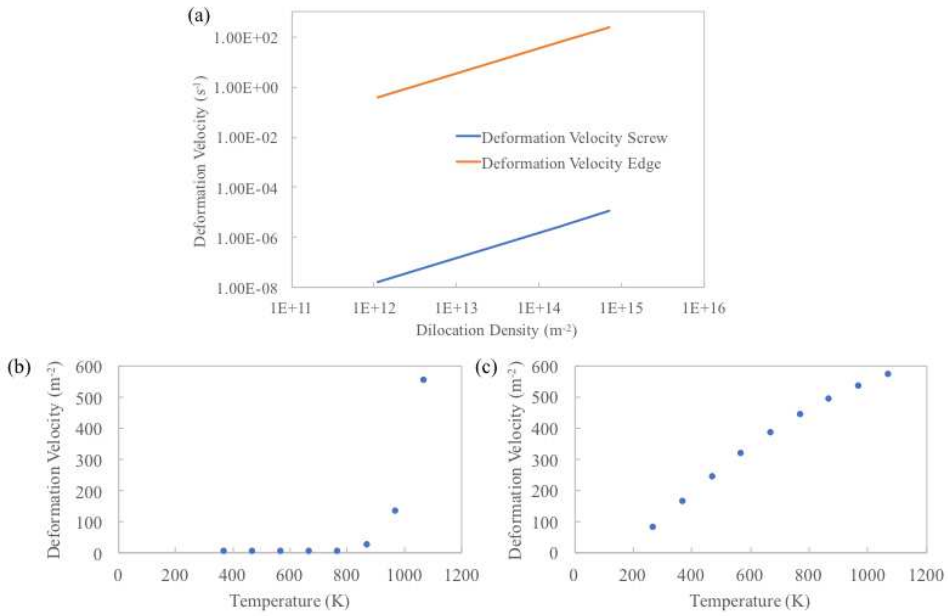

Figure 11 (a) Deformation velocity of tungsten with screw or edge dislocations as a function of dislocation density, (b) deformation velocity of tungsten with screw dislocations as a function of temperature, (c) deformation velocity of tungsten with edge dislocations as a function of temperature.

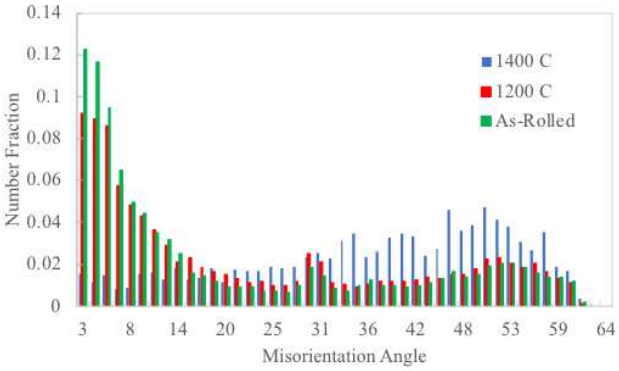
0.14
0.12
0.1
0.08
0.06
0.04
0.02
0
Number Fraction
1400 C
1200 C
As-Rolled
3
8
14
20
25
31
36
42
48
53
59
64
Misorientation Angle

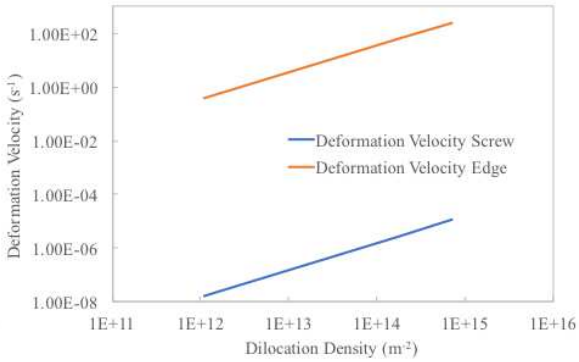
1.00E+02
1.00E+00
1.00E-02
1.00E-04
1.00E-06
1.00E-08
Deformation Velocity (s-1)
Deformation Velocity Screw
Deformation Velocity Edge
1E+11
1E+12
1E+13
1E+14
1E+15
1E+16
Dilocation Density (m-2)